Article | Received 15 June 2023; Accepted 7 August 2023; Published 17 August 2023
https://doi.org/10.55092/mt20230002

Improved adaptive-critic-based dynamic event-triggered control for non-affine systems

Zihang Zhou[1,2,3,4], Ao Liu[1,2,3,4], and Ding Wang[1,2,3,4,*]

[1]Faculty of Information Technology, Beijing University of Technology, Beijing 100124, China
[2]Beijing Key Laboratory of Computational Intelligence and Intelligent System, Beijing University of Technology, Beijing 100124, China
[3]Beijing Institute of Artificial Intelligence, Beijing University of Technology, Beijing 100124, China
[4]Beijing Laboratory of Smart Environmental Protection, Beijing University of Technology, Beijing 100124, China

* Correspondence author; E-mail: dingwang@bjut.edu.cn.

Abstract: In this paper, by employing a recurrent neural network and a critic neural network (CNN), we design an improved dynamic event-triggered controller for a class of non-affine continuous-time nonlinear systems. To address the transformation of the robust-optimal control problem, an additional utility function reflecting the disturbance is introduced. Besides, a system identifier is utilized for reconstructing the non-affine dynamics to generate an affine model. For reducing the waste of communication resources, a dynamic event-triggered control strategy is developed to replace the traditional time-based structure and improve static event-triggered control design. In addition, we develop an enhanced CNN weight updating law, which allows for greater flexibility in the process of weight selection compared to the conventional approach. The dynamic event-triggered controller is designed by using the CNN framework. Finally, a simulation of a modified torsional pendulum system is performed to demonstrate the effectiveness of the constructed method.

Keywords: adaptive critic learning; dynamic event-triggered control design; neural networks; non-affine dynamics; robust-optimal control; system identification

1. Introduction

Real-world controlled systems are often subject to environmental changes, external disturbances, and modeling errors, which can significantly impact the system stability and performance. As a result, achieving stabilization is crucial for the controller. To address this challenge, advanced techniques such as adaptive critic learning (ACL) have been developed to obtain approximate solutions of Hamilton-Jacobi-Bellman (HJB) equations, which are often too complex to be solved analytically [1–8]. ACL offers a notable advantage in effectively avoiding the "curse of dimensionality", which has traditionally plagued dynamic programming methods. Over the years, ACL has been applied in various fields, including tracking control design, adaptive optimal control design, differential games, and robust control successfully [9–14]. Recent development in adaptive and learning approaches has greatly expanded the scope of research in robust control. One of the most promising areas of research is the integration of optimal control and robust stabilization, which has attracted significant attention in recent years. The benefits of this approach are twofold: it not only ensures robustness in the presence of uncertainties and disturbances but also optimizes the control performance. In recent years, the combination of ACL design and traditional robust control has emerged as a promising approach to achieve both robustness and performance optimization. In [15], the connection between optimal control design and robust control problem was demonstrated. This led to the

development of an improved robust control design approach that combines advanced ACL with the traditional robust control method presented by Wang *et al.* [16]. However, there is still a need to further research to explore the design method of the robust controller for non-affine systems.

ACL is a control method that combines the principles of reinforcement learning, optimal control, and neural networks (NNs). NNs are an essential component of the ACL technique. They are used to approximate cost functions and control policies of the system. Different types of NNs are frequently used in ACL, including back-propagation NNs, feed-forward NNs, and recurrent NNs (RNNs), and so on. These NNs are simple but powerful tools for learning and controlling complex systems, especially in the presence of large amounts of data. The use of NNs in ACL opens up new opportunities for advanced control methods to expand the range of applications, including robotics, manufacturing, and aerospace engineering [17, 18]. In [19], an actor-critic NN was proposed to address the optimal control issue for continuous-time (CT) systems. However, in most cases, critic NNs (CNNs) are more convenient than actor-critic NNs for approximating nonlinear systems, as the former requires only one network to approximate both the cost function and the control law. For example, a critic NN was employed to approximate the cost function and the control law in [20]. This approach showed superior performance compared to other control methods in a simulation of a double inverted pendulum system. By using a single critic network, the computational burden can be reduced. Furthermore, the selection of initial weights is needed to investigate. Therefore, an improved critic network control strategy is established in this paper.

In practical applications, non-affine nonlinear plants are commonly encountered challenges due to their complex dynamics. The control law of an affine system can be represented directly, allowing for the construction of an optimal feedback controller. As a result, research efforts have mainly focused on affine systems. For instance, in the context of discrete-time nonzero-sum games based on nonlinear affine systems, the design of feedback controllers was explored by using off-policy integral reinforcement learning strategies [21]. Additionally, an adaptive critic approach with a novel event-based condition was proposed for CT affine nonlinear systems [22]. However, it is important to note that dynamics encompass both affine and non-affine systems. Non-affine systems have more general dynamical expressions and require corresponding feedback solutions. Several research methods based on ACL have been developed for non-affine systems, including robust stabilization through system identification techniques [23]. Nonetheless, few of authors consider the event-triggered control strategy for non-affine systems to reduce more communication and computational overhead.

The triggering mechanism allows for a significant reduction in communication and computational overhead, which is particularly important in resource-constrained systems. Several different triggering mechanisms have been proposed, such as time-based and event-based. Time-based methods use a predefined time interval to determine when to transmit control signals, while event-based methods use the deviation of system variables from their set-points to trigger transmission. One of the primary advantages of event-triggered control strategies (ETCSs) is the reduction in communication and computational overhead. This reduction results in lower energy consumption, longer system lifetimes, and increased system efficiency. Moreover, the use of ETCSs can improve the robustness of controlled systems by allowing them to adapt to changes in the environment, disturbances, and uncertainties. Overall, the development and application of ETCSs have attracted significant attention in recent years due to their potential for addressing numerous which are difficult to deal with by using traditional time-triggered control strategies. In [24], Yang *et al.* addressed the issue of nonlinear systems with asymmetric input constraints and proposed an adaptive-critic-based static event-triggered H_∞ control method. While static event-triggered control strategies (SETCSs) can reduce redundant transmission and the number of updating steps effectively, it is important to acknowledge that SETCSs still have room for improvement. Additionally, in [25], the concept

of an internal dynamic variable was proposed to enhance ETCSs. This approach, called the dynamic event-triggered control strategy (DETCS), utilizes an internal signal that can be non-monotonic and help improve the control performance. Recently, there has been a growing interest in the study of DETCSs. The DETCS has gained attention due to their potential of improving the control performance and reducing resource utilization in feedback control systems. By adjusting the triggering conditions dynamically, the DETCS can achieve a balance between control accuracy and communication/computation costs. In [26], a model-based dynamic event-triggered transmission strategy was proposed for linear systems. It provides a framework for designing intelligent and adaptive communication protocols in control systems, allowing for more efficient utilization of network resources and improved overall system performance. However, few DETCSs are used to study the non-affine nonlinear systems. It is the driving force behind this study. Thus, in this paper, we develop a novel DETCS for a class of non-affine systems. Besides, we consider the improved weight tuning rule and design the DETCS for reducing the communication and computational overhead.

The technical note is organized as follows. In Section 2, we provide a comprehensive discussion on the non-affine disturbed system and present the transformation of the robust-optimal control problem. In Section 3, the system identifier is constructed based on the RNN. In Section 4, we design the static and dynamic event-triggered optimal controllers. In Section 5, we design the improved weight tuning rule and realize event-triggered controllers based on the CNN. Moveover, the stability of the close-loop system is proved. In Section 6, a simulation example is used to show the effectiveness of the established method. In Section 7, the conclusion of the paper is presented.

Notations: $\mathbb{R}$ denotes the set of all real numbers. $\mathbb{R}^n$, $\mathbb{R}^m$, and $\mathbb{R}^\Upsilon$ represent the Euclidean space which are n-dimensional, m-dimensional, and Υ-dimensional. $\mathbb{R}^{n\times n}$, $\mathbb{R}^{m\times m}$, and $\mathbb{R}^{\Upsilon\times m}$ indicate $n\times n$ real matrices, $m\times m$ real matrices, and $\Upsilon\times m$ real matrices respectively. $\|\cdot\|$ represents the vector norm or the matrix norm. $\mathbb{C}(\Omega)$ is the set of admissible control laws on Ω. $\nabla(\cdot)$ denotes the gradient computation and T is the transpose operation. $\lambda_{\min}(\cdot)$ is the minimal eigenvalue of a matrix.

2. Design basis for robustness guarantee

Consider a category of CT nonlinear non-affine plants as

$$\dot{x}(t) = \mathscr{A}_n(x(t),u(t)),\ \ x(0) = x_0, \tag{1}$$

where $x(t)\in\mathbb{R}^n$ is the state vector and $u(t)\in\mathbb{R}^m$ is the control matrix. $\mathscr{A}_n(\cdot,\cdot)$ is the unknown infinitely differentiable function, which is assumed to be Lipschitz continuous on the set $\Omega\subset\mathbb{R}^n$ containing the origin $\mathscr{A}_n(0,0)=0$, and $x(0)$ is the initial value of the state. Assume the system (1) is controllable.

It is worth noting that disturbances exist widely in practical applications. If the system (1) is affected by disturbances, it can be written as

$$\dot{x} = \mathscr{A}_n(x,u) + d(x), \tag{2}$$

where $d(x)\in\mathbb{R}^n$ represents the unknown perturbation term with $d(0)=0$, and $\|d(x)\|\le\lambda_d(x)$ with $\lambda_d(0)=0$. Note that $x(t)$ and $u(t)$ can be briefly written as x and u.

Then, we delve into the robust-optimal problem transformation. To construct the infinite horizon integral cost function for the nominal system (1), we can proceed as follows:

$$\mathscr{J}(x) = \int_t^\infty (U(x(\tau),u(\tau)) + U_d(x(\tau),u(\tau)))\mathrm{d}\tau,\ \mathscr{J}(0)=0 \tag{3}$$

where $U(x,u)\ge 0$ is the basis utility term with $U(0,0)=0$, and $U_d(x,u)\ge 0$ is the additional utility denoting the perturbation.

We select an admissible control law $u(x)$ to derive the nonlinear Lyapunov equation as

$$0 = U(x,u) + U_d(x,u) + (\nabla \mathscr{J}(x))^{\mathsf{T}} \mathscr{A}_n(x,u), \tag{4}$$

The Hamiltonian function is

$$H(x,u(x),\nabla \mathscr{J}(x)) = U(x,u) + U_d(x,u) + (\nabla \mathscr{J}(x))^{\mathsf{T}} \mathscr{A}_n(x,u). \tag{5}$$

Thus, the definition of the optimal cost function can be described as

$$\mathscr{J}^*(x) = \min_{u(x)\in\mathbb{C}(\Omega)} \int_t^{\infty} (U(x(\tau),u(\tau)) + U_d(x(\tau),u(\tau)))\mathrm{d}\tau. \tag{6}$$

Then, we can have the corresponding HJB equation

$$0 = \min_{u(x)\in\mathbb{C}(\Omega)} H(x,u(x),\nabla \mathscr{J}^*(x)), \tag{7}$$

where $u^*(x)$ denotes the optimal control law, and it represents

$$u^*(x) = \arg\min_{u\in\mathbb{C}(\Omega)} H(x,u(x),\nabla \mathscr{J}^*(x)). \tag{8}$$

This difficulty is compounded for non-affine systems since expressing the optimal solution directly is extremely difficult. Furthermore, the specific form of $U_d(x)$ is often unknown. We use $u^*(x)$ as the optimal control law and add an additional utility term $U_d(x)$

$$U_d(x) = \frac{1}{4}(\nabla \mathscr{J}^*(x))^{\mathsf{T}} \nabla \mathscr{J}^*(x) + \lambda_d^2(x). \tag{9}$$

It is important to note that $U_d(x)$ plays a significant role in the theoretical interpretation of optimal-robust problems transformation, despite the fact that the optimal cost function is not known beforehand. Moreover, the positive definite form of $U_d(x)$ facilitates easy determination of asymptotic stability. In practice, estimated values can be used during implementation.

Theorem 1 *Considering the cost function* (3) *and utility term* (9)*, we can ensure robust stability for the disturbed system* (2) *by using the optimal feedback control law* $u^*(x)$*, which guarantees asymptotic stability.*

Proof. Suppose $\mathscr{L}_d(t)$ is a Lyapunov function and set $\mathscr{J}^*(x) = \mathscr{L}_d(t)$. Then we can obtain the derivative $\dot{\mathscr{L}}_d(t) = \mathrm{d}\mathscr{L}_d(t)/\mathrm{d}t$ as

$$\begin{aligned}\dot{\mathscr{L}}_d(t) =& (\nabla \mathscr{J}^*(x))^{\mathsf{T}} [\mathscr{A}_n(x,u^*(x)) + d(x)] \\ =& -\frac{1}{4}(\nabla \mathscr{J}^*(x))^{\mathsf{T}} \nabla \mathscr{J}^*(x) - \lambda_d^2(x) - U(x,u^*(x)) + (\nabla \mathscr{J}^*(x))^{\mathsf{T}} d(x).\end{aligned} \tag{10}$$

For $\|d(x)\| \le \lambda_d(x)$, we have

$$\begin{aligned}\dot{\mathscr{L}}_d =& -\lambda_d^2(x) + d^{\mathsf{T}}(x)d(x) - U(x,u^*(x)) - \left[\frac{1}{2}\nabla \mathscr{J}^*(x) - d(x)\right]^{\mathsf{T}} \left[\frac{1}{2}\nabla \mathscr{J}^*(x) - d(x)\right] \\ \le& -U(x,u^*(x)).\end{aligned} \tag{11}$$

Based on $U(x,u^*(x)) \ge 0$, the conclusion that $\dot{\mathscr{L}}_d \le 0$ is clear. Since $U(x,u^*(x)) > 0$ for all $x \ne 0$, we can infer that $\dot{\mathscr{L}}_d < 0$. This finding confirms that the closed-loop system exhibits asymptotic stability, thus completing the proof. ■

Indeed, the optimal control solution for the nominal system is crucial in ensuring the robustness of nonlinear systems with disturbances. In the subsequent section, we present the design of a system identifier utilizing a RNN based on this theoretical framework.

3. Recurrent-Neural-Network-Based system identifier design

For the nominal plant of the non-affine system (1), it can be learned in an affine norm as

$$\dot{x}(t) = \mathscr{A}(x(t), u(t)). \tag{12}$$

In order to simplify the mathematical model and enhance computational efficiency, we have developed an RNN-based system identifier to learn the unknown dynamics of the nonlinear system. By employing the RNN framework proposed in [27], we can reformulate the original system (1) as

$$\mathscr{A}_n(x,u) = w_{r1}x + w_{r2}\delta_r(x) + w_{r3} + Cu + e_r(t), \tag{13}$$

where $\delta_r(x) = \tanh(D^{\mathsf{T}}X)$ is the activation function with $D \in \mathbb{R}^{\Upsilon \times n}$, and X is explained in (14). $w_{r1} \in \mathbb{R}^{n\times n}$, $w_{r2} \in \mathbb{R}^{n\times n}$, and $w_{r3} \in \mathbb{R}^n$ are ideal weight matrices, $C \in \mathbb{R}^{n\times m}$ is the ideal control coefficient matrix, and $e_r(t) \in \mathbb{R}^n$ is the approximate NN error vector. The operation is denoted as

$$X = \Xi(X_m) = \overbrace{\left[\chi_m^{\mathsf{T}}, \ldots, \chi_m^{\mathsf{T}}\right]^{\mathsf{T}}}^{\Upsilon} \in \mathbb{R}^{\Upsilon}, \tag{14}$$

where $X_m = x \otimes I_q$, I_q is the identity matrix, "$\otimes$" represents the Kronecker product. Besides, by using the reconstructed model (13), the nominal non-affine system (1) can be formulated in the following affine form:

$$\dot{x} = \mathscr{A}_n(x,u) = f(x) + Cu, \tag{15}$$

The utility term is selected as $U = x^{\mathsf{T}}Qx + u^{\mathsf{T}}Ru$ for simplicity, where Q and R are all positive definite matrices with suitable dimensions. Thus, the optimal control law is $u^*(x) = (-1/2)R^{-1}C^{\mathsf{T}}\nabla \mathscr{J}^*(x)$. The corresponding approximation of (13) is

$$\dot{\hat{x}} = \hat{w}_{r1}\hat{x} + \hat{w}_{r2}\tanh\left(\hat{D}^{\mathsf{T}}\hat{X}\right) + \hat{w}_{r3} + \hat{C}u + \varepsilon\tilde{x}, \tag{16}$$

where $\hat{x} \in \mathbb{R}^n$ is the estimated state, $\hat{C}$ is the estimated control coefficient matrix with respect to weights, and $\hat{w}_{r1}, \hat{w}_{r2}, \hat{w}_{r3}$, $\hat{X}$ and $\hat{D}$ are estimated matrices with same dimensions as (13). Note that $\varepsilon\tilde{x}$ is the robust feedback term, where ε is a designed parameter, and $\tilde{x} = x - \hat{x}$ is the state identification error with $\dot{\tilde{x}} = \dot{x} - \dot{\hat{x}}$.

Theorem 2 *As to the established identifier model (13), the estimated weight matrices are trained as*

$$\dot{\hat{w}}_{r1} = a_1\tilde{x}\hat{x}^{\mathsf{T}}, \tag{17}$$

$$\dot{\hat{w}}_{r2} = a_2\tanh(\hat{D}^{\mathsf{T}}\hat{X})\tilde{x}^{\mathsf{T}}, \tag{18}$$

$$\dot{\hat{w}}_{r3} = a_3\tilde{x}, \tag{19}$$

$$\dot{\hat{C}} = a_4\tilde{x}u^{\mathsf{T}}, \tag{20}$$

$$\dot{\hat{D}} = a_5\tilde{x}\tilde{x}^{\mathsf{T}}, \tag{21}$$

where $a_{i_v} > 0$ is the learning rate, $i_v = 1,2,3,4,5$, and the corresponding identification error is asymptotically stable.

Remark 1 *The relevant proof here has been presented in [27], and we do not provide any further proof.*

From Theorem 2, the identifier (16) is asymptotically stable under learning laws (17)–(21). When $\tilde{x}$ tends to 0, $\dot{\hat{w}}_{ri}$ with $i = 1,2,3$, $\dot{\hat{C}}$, and $\dot{\hat{D}}$ can tend to 0. Consequently, the nominal model of (1) after sufficient learning process can be written as follows:

$$\dot{\hat{x}} = \hat{w}_{r1}\hat{x} + \hat{w}_{r2}\tanh(\hat{D}^{\mathsf{T}}\hat{X}) + \hat{w}_{r3} + \hat{C}u. \tag{22}$$

The above expression (22) can be more simple as

$$\dot{x} = \hat{f}(x) + \hat{C}u, \tag{23}$$

where $\hat{f}(x) = \hat{w}_{r1}\hat{x} + \hat{w}_{r2}^{\mathsf{T}}\tanh(\hat{D}^{\mathsf{T}}\hat{X}) + \hat{w}_{r3}$. Thus, with the obtained reconstruction model, further analysis can be carried out accordingly. For ease of understanding, we simplify its expression to $\dot{x} = f(x) + Cu$ in the following section. According to this expression, the Hamiltonian function (5) becomes

$$H(x,u(x),\nabla\mathscr{J}(x)) = U(x,u) + U_d(x,u) + (\nabla\mathscr{J}(x))^{\mathsf{T}}(f(x) + Cu). \tag{24}$$

4. Event-Triggered optimal control design

Considering the limitation of computation and communication bandwidths, the ETCS is developed. $\{c_j\}_{j=0}^{\infty}$ is a monotonically increasing sequence of triggering instants, where c_j is the jth consecutive sampling instant with $j \in \mathbb{N}$. Then, the output of the sampled-data component is a sequence of the sampled state represented as $x(c_j) \triangleq \widehat{x}_j$ for all $t \in [c_j, c_{j+1})$. We define the error function between the current state and the sampled state as

$$e_j = \widehat{x}_j - x, \forall t \in [c_j, c_{j+1}). \tag{25}$$

Through a zero-order hold, we obtain that $u(x(c_j)) = u(\widehat{x}_j) \triangleq \mu(\widehat{x}_j), \forall t \in [c_j, c_{j+1})$. The sampled state becomes

$$\dot{x} = f(x) + C\mu(\widehat{x}_j), \forall t \in [c_j, c_{j+1}). \tag{26}$$

Then, the optimal control law based on events is

$$\mu^*(\widehat{x}_j) = -\frac{1}{2}R^{-1}C^{\mathsf{T}}\nabla\mathscr{J}^*(\widehat{x}_j). \tag{27}$$

Stemmed from the event-based optimal control law (27), the Hamiltonian function is

$$\begin{aligned} &H(x,\mu^*(\widehat{x}_j),\nabla\mathscr{J}^*(x)) \\ &= U_d + x^{\mathsf{T}}Qx + (\nabla\mathscr{J}^*(x))^{\mathsf{T}}f(x) - \frac{1}{2}(\nabla\mathscr{J}^*(x))^{\mathsf{T}}CR^{-1}C^{\mathsf{T}}\nabla\mathscr{J}^*(\widehat{x}_j) \\ &\quad + \frac{1}{4}(\nabla\mathscr{J}^*(\widehat{x}_j))^{\mathsf{T}}CR^{-1}C^{\mathsf{T}}\nabla\mathscr{J}^*(\widehat{x}_j). \end{aligned} \tag{28}$$

In order to further proceed, it is necessary to make an assumption that has been used in [11]

Assumption 1 *Assume that the control law $u(x)$ satisfies Lipschitz continuity, which means $\|u(x) - \mu(\widehat{x}_j)\| \le K_{u_e}\|e_j\|$ holding, where K_{u_e} is a positive constant.*

Theorem 3 *Assuming that Assumption 1 is satisfied, the application of the event-triggered control law given by the equation* (27)*, along with the cost function* (3)*, ensures the stability of the controlled system. The static event-triggered condition can be expressed as*

$$\begin{aligned} \|e_j\|^2 &\le \frac{(1-\theta_1^2)\lambda_{\min}(Q)\|x\|^2 + (1-2\|r\|^2)\lambda_d^2(x)}{2\|r\|^2K_{u_e}^2} \\ &\triangleq \|e_{T_s}\|^2, \end{aligned} \tag{29}$$

where $\theta_1 > 0$, $r = \sqrt{R}$, and e_{T_s} is the SETC threshold.

Proof. For demonstrating that $\mu^*(\widehat{x}_j)$ is a solution to the robust stabilization problem, the Lyapunov function is selected as $\mathscr{L}_{e_T}(t) = \mathscr{J}^*(x)$. On the basis of the definition of $\mathscr{J}^*(x)$, $\forall x \neq 0$, $\mathscr{J}^*(x) > 0$, and $\mathscr{J}^*(0) = 0$, it can be concluded that $\mathscr{L}_{e_T}(t)$ is positive definite. By taking the derivative of the Lyapunov function $\mathscr{L}_{e_T}(t)$ along the trajectory of the system (2) and the disturbed nominal dynamics $\dot{x} = f(x) + Cu + d(x)$, we can obtain that

$$\dot{\mathscr{L}}_{e_T}(t) = (\nabla \mathscr{J}^*(x))^{\mathsf{T}}(f(x) + C\mu^*(\widehat{x}_j) + d(x)). \tag{30}$$

Then, according to the time-based optimal law $u^*(x) = -(1/2)R^{-1}C^{\mathsf{T}}\nabla \mathscr{J}^*(x)$ and the Hamiltonian function (24), we can derive that

$$(\nabla \mathscr{J}^*(x))^{\mathsf{T}} f(x) = -U_d(x) - x^{\mathsf{T}}Qx + u^{*\mathsf{T}}Ru^*. \tag{31}$$

Combining the time-based $u^*(x)$ and (31), (30) can be rewritten as

$$\dot{\mathscr{L}}_{e_T}(t) = -x^{\mathsf{T}}Qx - U_d(x) - (\mu^*(\widehat{x}_j) + d(x))^{\mathsf{T}}R(\mu^*(\widehat{x}_j) + d(x)) + \pi_e^{\mathsf{T}}R\pi_e, \tag{32}$$

where $\pi_e = u^* - \mu^*(\widehat{x}_j) - d(x)$. Then, $\pi_e^{\mathsf{T}}R\pi_e = (r\pi_e)^{\mathsf{T}}(r\pi_e) = \|r\pi_e\|^2$. Considering $\|d(x)\| \leq \lambda_d(x)$ and Assumption 1, we can obtain that

$$\pi_e^{\mathsf{T}}R\pi_e \leq \|r\|^2\left\|u^*(x) - \mu^*(\widehat{x}_j) - d(x)\right\|^2 \leq 2\|r\|^2(K_{ue}^2\left\|e_j\right\|^2 + \lambda_d^2(x)). \tag{33}$$

Moreover,

$$\begin{aligned}\dot{\mathscr{L}}_{e_T}(t) &\leq -\lambda_{\min}(Q)\|x\|^2 - \lambda_d^2(x) + 2\|r\|^2(K_{ue}^2\left\|e_j\right\|^2 + \lambda_d^2(x)) \\ &= -(1-\theta_1^2)\lambda_{\min}(Q)\|x\|^2 - \theta_1^2\lambda_{\min}(Q)\|x\|^2 + 2\|r\|^2K_{ue}^2\left\|e_j\right\|^2 + (2\|r\|^2 - 1)\lambda_d^2(x).\end{aligned} \tag{34}$$

Therefore, if the SETC rule (29) holds, $\dot{\mathscr{L}}_{e_T}(t) \leq -\theta_1^2\lambda_{\min}(Q)\|x\|^2 < 0, \forall x \neq 0$ is true. Then, conditions for Lyapunov local stability theory can be satisfied. We can have the conclusion that the closed-loop system achieves asymptotic stability. ■

In this paper, it needs to introduce an internal dynamic variable $\eta(x)$, which can be used to improve the effect of the SETCS. We define that

$$\dot{\eta}(x) = (1-\theta_1^2)\lambda_{\min}(Q)\|x\|^2 + (1-2\|r\|^2)\lambda_d^2(x) - 2\|r\|^2K_{u_e}^2\left\|e_j\right\|^2 - \alpha\eta(x), \tag{35}$$

where $\eta(x) \geq 0$. $\alpha \in \mathbb{R}$ is the additional designed positive parameter.

Theorem 4 *Theorem 2 guarantees asymptotic stability of the closed-loop system. Additionally, the dynamic event-based control condition for the system* (1) *can be expressed as follows:*

$$\left\|e_j\right\|^2 \leq \frac{\eta(x)}{2\alpha_d\|r\|^2K_{u_e}^2} + \|e_{T_s}\|^2 \triangleq \|e_{T_d}\|^2, \tag{36}$$

where $\alpha_d \in \mathbb{R}$ is the designed parameter of the internal dynamic variable $\eta(x)$ and e_{T_d} is the DETC threshold.

Proof. The proof procedure for this result is similar to Theorem 3. We select a Lyapunov function $\mathscr{L}_{e_{T_d}}(t) = \mathscr{J}^*(x) + \eta(x)$, and use the conclusion established in Theorem 3 to demonstrate

$$\begin{aligned}\dot{\mathscr{L}}_{e_{T_d}}(t) &\leq -U_d(x) - x^{\mathsf{T}}Qx - \dot{\eta}(x) + 2\|r\|^2(K_{u_e}^2\left\|e_j\right\|^2 + \lambda_d^2(x)) \\ &\leq -\alpha\eta(x) - \theta_1^2\lambda_{\min}(Q)\|x\|^2.\end{aligned} \tag{37}$$

Note that $\dot{\mathscr{L}}_{e_{T_d}}(t) < 0$ and $\eta(x)$ converges to the origin, satisfying conditions for Lyapunov local stability theory. Then, the proof is completed. ■

Remark 2 *When α_d tends to $+\infty$, the static event-triggered control threshold* (29) *can be regarded as a limited case of the condition* (36).

5. Event-Triggered Critic-Neural-Network-Based control implementation

5.1. Weight learning rule of the critic network

The optimal cost function $\mathscr{J}^*(x)$ is reconstructed on a compact set Ω using a-hidden-layer NN with n_c neurons as

$$\mathscr{J}^*(x) = w_c^{\mathsf{T}} \delta_c(x) + e_c(x), \tag{38}$$

where $w_c \in \mathbb{R}^{n_c}$ represents the ideal unknown weight vector, $\delta_c(x) \in \mathbb{R}^{n_c}$ denotes the activation function vector, and $e_c(x) \in \mathbb{R}$ is the reconstruction error. Then, we obtain the gradient vector $\nabla \mathscr{J}^*(x) = (\nabla \delta_c(x))^{\mathsf{T}} w_c + \nabla e_c(x)$. The optimal cost function is approximated as

$$\hat{\mathscr{J}}^*(x) = \hat{w}_c^{\mathsf{T}} \delta_c(x), \tag{39}$$

where $\hat{w}_c \in \mathbb{R}^{n_c}$ is the estimated weight vector, and $\nabla \hat{\mathscr{J}}^*(x) = (\nabla \delta_c(x))^{\mathsf{T}} \hat{w}_c$. The approximate event-based optimal control law becomes

$$\hat{\mu}^*(\hat{x}_j) = -\frac{1}{2} R^{-1} C^{\mathsf{T}} (\nabla \delta_c(\hat{x}_j))^{\mathsf{T}} \hat{w}_c. \tag{40}$$

Thus, the Hamiltonian function (24) is changed into

$$\begin{aligned} \hat{H}(x, \hat{\mu}^*(\hat{x}_j), \hat{w}_c) &= U(x, \hat{\mu}^*(\hat{x}_j)) + U_d(x) + \hat{w}_c^{\mathsf{T}} \nabla \delta_c(x)(f(x) + C\hat{\mu}^*(\hat{x}_j)) \\ &\triangleq \varepsilon_h. \end{aligned} \tag{41}$$

The object of training the weight $\hat{w}_c$ is to minimize $E_c = 0.5\varepsilon_h^2$. One needs an initial admissible control law to begin the process of learning, but the search for such a controller is challenging. To overcome this difficulty, an assumption can be made, and an extra term can be introduced to enhance the learning process.

Assumption 2 *Let $\mathscr{J}_L(x)$ be a continuously differentiable Lyapunov function candidate that satisfies a certain formula [28]. It is relevant to the nominal form* (23)*, the feedback control law $u^*(x)$, and the corresponding Hamiltonian function* (24) *of the system* (1).

$$\dot{\mathscr{J}}_L(x) = (\nabla \mathscr{J}_L(x))^{\mathsf{T}} (f(x) + Cu^*(x)) < 0. \tag{42}$$

By selecting a positive definite matrix $\mathscr{K} \in \mathbb{R}^{2n \times 2n}$, it is possible to ensure that the inequality

$$(\nabla \mathscr{J}_L(x))^{\mathsf{T}} (f(x) + Cu^*(x)) = -(\nabla \mathscr{J}_L(x))^{\mathsf{T}} \mathscr{K} \nabla \mathscr{J}_L(x) \leq -\lambda_{\min}(\mathscr{K}) \|\nabla \mathscr{J}_L(x)\|^2 \tag{43}$$

holds. It is noteworthy that during implementation, $\mathscr{J}_L(x)$ can be obtained by selecting an appropriate polynomial of the state vector, such as $\mathscr{J}_L(x) = 0.25x^{\mathsf{T}}x$.

In this paper, we adopt an improved weight leaning law, which is presented below:

$$\begin{aligned} \dot{\hat{w}}_c &= -\varsigma \frac{\Im}{(1+\Im)^2} \frac{\partial E_c}{\partial \hat{w}_c} + \frac{1}{2} \alpha_L \nabla \delta_c(x) C R^{-1} C^{\mathsf{T}} \nabla \mathscr{J}_L(x) \\ &= -\varsigma \frac{\sigma \Im}{(1+\Im)^2} (U(x, \hat{\mu}^*(\hat{x}_j)) + U_d(x) + \sigma^{\mathsf{T}} \hat{w}_c) + \frac{1}{2} \alpha_L \nabla \delta_c(x) C R^{-1} C^{\mathsf{T}} \nabla \mathscr{J}_L(x), \end{aligned} \tag{44}$$

where $\varsigma \in (0,1)$ denotes the learning rate, $\sigma = \nabla \delta_c(x)(f(x) + C\hat{\mu}^*(\hat{x}_j))$ is an n_c-dimensional column vector. Let $\sigma^{\mathsf{T}}\sigma = \Im$. It is obviously that $\Im > 0$. α_L represents the adjusting rate for the additional stabilizing term. Compared to the conventional updating rule, a more robust structure is introduced with two adjustable learning rates ς and α_L in the improved tuning law

(44). As a result, we can tackle practical control tasks based on their engineering intuition and experience.
If we define the weight error vector as $\tilde{w}_c = w_c - \hat{w}_c$, then it follows that $\dot{\tilde{w}}_c = -\dot{\hat{w}}_c$. Further details are provided as follows:

$$\begin{aligned}\dot{\tilde{w}}_c =& \varsigma \frac{\Im}{(1+\Im)^2}\frac{\partial E_c}{\partial \hat{w}_c} - \frac{1}{2}\alpha_L \nabla \delta_c(x) C R^{-1} C^{\mathsf{T}} \nabla \mathscr{J}_L(x) \\ =& -\varsigma \frac{\sigma \Im}{(1+\Im)^2}(\sigma^{\mathsf{T}} \tilde{w}_c - \varpi) - \frac{1}{2}\alpha_L \nabla \delta_c(x) C R^{-1} C^{\mathsf{T}} \nabla \mathscr{J}_L(x),\end{aligned} \tag{45}$$

where $\varpi = -(\nabla e_c(x))^{\mathsf{T}}(f(x) + C\hat{\mu}^*(\widehat{x}_j))$ is the residual error. The next section is based on the improved weight tuning law to realize the design for event-based controllers. The relevant proof is provided in the next section.

5.2. Static Event-Triggered Neural-Network-Based controller design

Then, we make the following assumption, which is used in [29].

Assumption 3 *The gradient of the activation function is Lipschitz continuous such that* $\|\nabla \delta_c(x) - \nabla \delta_c(\widehat{x}_j)\| \le K_{\delta_c} \|e_j\|$, *where* $K_{\delta_c} > 0$. *The gradient of the activation function, the gradient of the reconstruction error, and the residual error are all bounded, i.e.,* $\|\nabla \delta_c(x)\| \le \lambda_1$, $\|\nabla e_c\| \le \lambda_2$, *and* $|\varpi| < \lambda_3$, *where* $\lambda_{i_m} > 0, i_m = 1,2,3$.

Theorem 5 *Based on Assumption 3, the closed-loop system is asymptotically stable and the corresponding weight error is uniformly ultimately bounded(UUB). The static triggering rule based on the critic network can be denoted as*

$$\begin{aligned}\|e_j\|^2 \le& \frac{(1-\theta^2)\lambda_{\min}(Q)\|x\|^2 + \|r\hat{\mu}^*(\widehat{x}_j)\|^2}{\xi_{s1} K_{\delta_c} \|\hat{w}_c\|^2} + \frac{(\nabla \hat{\mathscr{J}}^*(x))^{\mathsf{T}} \nabla \hat{\mathscr{J}}^*(x)}{4\xi_{s1} K_{\delta_c} \|\hat{w}_c\|^2} \\ \triangleq& \|\hat{e}_{T_s}\|^2,\end{aligned} \tag{46}$$

and the inequality of the weight error is

$$\|\tilde{w}_c\| > \sqrt{\frac{\xi_{s3}}{\xi_{s2}}}, \tag{47}$$

where $\|\hat{e}_{T_s}\|$ *is the SETC threshold based on the critic network,* $\theta \in (0,1)$ *is a designed parameter to adjust the triggering condition,* $\xi_{s1} = (1/2)\|r\|^2 \|R^{-1}\|^2 \|C\|^2$, $\xi_{s2} = \Im \lambda_{\min}(\sigma\sigma^{\mathsf{T}}) \big/ 2(1+\Im)^2 - 2\xi_{s1}\lambda_1^2$, *and* $\xi_{s3} = \varsigma \Im \lambda_2^2 \big/ 2(1+\Im)^2 + 2\xi_{s1}\lambda_2^2$.

Proof. We choose a Lyapunov function $\mathscr{L}_s(t) = \mathscr{L}_{s_1}(t) + \mathscr{L}_{s_2}(t) + \mathscr{L}_{s_3}(t)$. More details are as follows:

$$\begin{aligned}\mathscr{L}_{s_1}(t) &= \mathscr{J}^*(x), \\ \mathscr{L}_{s_2}(t) &= \mathscr{J}^*(\widehat{x}_j), \\ \mathscr{L}_{s_3}(t) &= \frac{1}{2\varsigma}\tilde{w}_c^{\mathsf{T}} \tilde{w}_c + \frac{\alpha_L}{\varsigma}\mathscr{J}_L(x).\end{aligned} \tag{48}$$

It is noteworthy that the considered system is an impulsive system. During the time interval $t \in [c_j, c_{j+1})$, no events are triggered. Instead, events are only triggered at $t = c_{j+1}$. *Case 1:* For $t \in [c_j, c_{j+1})$, events are not triggered. Calculating the time derivative of $\mathscr{L}_s$ along the

trajectory, we can find that

$$\begin{aligned}\dot{\mathscr{L}}_{s_1} &= (\nabla \mathscr{J}^*(x))^{\mathsf{T}}(f(x)+C\hat{\mu}(\hat{x}_j)),\\ \dot{\mathscr{L}}_{s_2} &= 0,\\ \dot{\mathscr{L}}_{s_3} &= \frac{1}{\varsigma}\tilde{w}_c^{\mathsf{T}}\dot{\tilde{w}}_c+\frac{\alpha_L}{\varsigma}(\nabla \mathscr{J}_L(x))^{\mathsf{T}}\dot{x}.\end{aligned} \tag{49}$$

For the term $\dot{\mathscr{L}}_{31}(t)$, based on (24) and the optimal control law $u^*(x)$, it becomes

$$\begin{aligned}\dot{\mathscr{L}}_{s_1}(t) &= -\frac{1}{4}(\nabla \hat{\mathscr{J}}^*(x))^{\mathsf{T}}\nabla \hat{\mathscr{J}}^*(x)-\lambda_d^2(x)-x^{\mathsf{T}}Qx+u^{*\mathsf{T}}(x)Ru^*(x)-2u^{*\mathsf{T}}(x)R\hat{\mu}^*(\widehat{x}_j)\\ &\leq -\frac{1}{4}(\nabla \hat{\mathscr{J}}^*(x))^{\mathsf{T}}\nabla \hat{\mathscr{J}}^*(x)-\lambda_d^2(x)-x^{\mathsf{T}}Qx-\|r\hat{\mu}(\widehat{x}_j)\|^2+\|r\|^2\|u^*(x)-\hat{\mu}^*(\widehat{x}_j)\|^2.\end{aligned} \tag{50}$$

We continue to analyse the term $\|u^*(x)-\hat{\mu}^*(\widehat{x}_j)\|^2$. The estimated time-based control optimal control law with regard to the approximated cost function is

$$u^*(x) = -\frac{1}{2}R^{-1}C^{\mathsf{T}}((\nabla\delta_c(x))^{\mathsf{T}}w_c+\nabla e_c(x)). \tag{51}$$

Besides, we have

$$\begin{aligned}&\left\|u^*(x)-\hat{\mu}^*(\widehat{x}_j)\right\|^2\\ &\leq \frac{1}{2}\left\|R^{-1}C^{\mathsf{T}}((\nabla\delta_c(\widehat{x}_j))^{\mathsf{T}}-(\nabla\delta_c(x))^{\mathsf{T}})\hat{w}_c\right\|^2+\frac{1}{2}\left\|R^{-1}C^{\mathsf{T}}((\nabla\delta_c(x))^{\mathsf{T}}\tilde{w}_c+\nabla e_c(x))\right\|^2.\end{aligned} \tag{52}$$

Then, according to Assumption 3, we can derive

$$\|\nabla\delta_c(x)-\nabla\delta_c(\widehat{x}_j)\|^2 \leq K_{\delta_c}^2\left\|e_j\right\|^2, \tag{53}$$

$$\left\|(\nabla\delta_c(x))^{\mathsf{T}}\tilde{w}_c+\nabla e_c(x)\right\|^2 \leq 2(\lambda_1^2\|\tilde{w}_c\|^2+\lambda_2^2). \tag{54}$$

The term $\dot{\mathscr{L}}_{s_1}(t)$ can be written as

$$\begin{aligned}\dot{\mathscr{L}}_{s_1}(t) \leq &-\frac{1}{4}(\nabla \hat{\mathscr{J}}^*(x))^{\mathsf{T}}\nabla \hat{\mathscr{J}}^*(x)-\lambda_d^2(x)-\lambda_{\min}(Q)\|x\|^2-\|r\hat{\mu}^*(\widehat{x}_j)\|^2\\ &+\frac{1}{2}\|r\|^2\|R^{-1}\|^2\|C\|^2(K_{\delta_c}^2\left\|e_j\right\|^2\|\hat{w}_c\|^2+2\lambda_1^2\|\tilde{w}_c\|^2+2\lambda_2^2).\end{aligned} \tag{55}$$

Considering (45), the term $\mathscr{L}_{s3}$ becomes

$$\begin{aligned}\dot{\mathscr{L}}_{s_3} =&-\frac{\tilde{w}_c^{\mathsf{T}}\sigma\Im\sigma^{\mathsf{T}}\tilde{w}_c}{(1+\Im)^2}+\frac{\tilde{w}_c^{\mathsf{T}}\sigma\Im\varpi}{(1+\Im)^2}-\frac{\tilde{w}_c^{\mathsf{T}}\alpha_L\nabla\delta_c(x)CR^{-1}C^{\mathsf{T}}\nabla \mathscr{J}_L(x)}{2\varsigma}+\frac{\alpha_L(\nabla \mathscr{J}_L(x))^{\mathsf{T}}}{\varsigma}\dot{x}\\ \leq&\frac{\Im}{2(1+\Im)^2}(\varpi^2-\tilde{w}_c^{\mathsf{T}}\sigma\sigma^{\mathsf{T}}\tilde{w}_c)-\frac{\tilde{w}_c^{\mathsf{T}}\alpha_L\nabla\delta_c(x)CR^{-1}C^{\mathsf{T}}\nabla \mathscr{J}_L(x)}{2\varsigma}+\frac{\alpha_L(\nabla \mathscr{J}_L(x))^{\mathsf{T}}}{\varsigma}\dot{x}.\end{aligned} \tag{56}$$

According to Assumptions 2, 3, and (23), we can derive

$$\begin{aligned}\dot{\mathscr{L}}_{s_3} \leq & \frac{\Im}{2(1+\Im)^2}(\lambda_3^2-\lambda_{\min}(\sigma\sigma^{\mathsf{T}})\|\tilde{w}_c\|^2)+\frac{\alpha_L(\nabla \mathscr{J}_L(x))^{\mathsf{T}}}{\varsigma}(f(x)+Cu^*(x))\\ &+\frac{\alpha_L(\nabla \mathscr{J}_L(x))^{\mathsf{T}}CR^{-1}C^{\mathsf{T}}\nabla e_c(x)}{2\varsigma}\\ \leq & \frac{\Im}{2(1+\Im)^2}(\lambda_3^2-\lambda_{\min}(\sigma\sigma^{\mathsf{T}})\|\tilde{w}_c\|^2)-\frac{\alpha_L}{\varsigma}\lambda_{\min}(\mathscr{K})\|\nabla \mathscr{J}_L(x)\|^2\\ &+\frac{\alpha_L}{2\varsigma}\|\nabla \mathscr{J}_L(x)\|\,\|C\|^2\left\|R^{-1}\right\|\lambda_2, \end{aligned} \tag{57}$$

where $\lambda_{\min}(\sigma\sigma^{\mathsf{T}})>0$, and $\lambda_{\min}(\cdot)$ denotes the minimal eigenvalue of a matrix. Furthermore, we have

$$\begin{aligned}\dot{\mathscr{L}}_s=&\sum_{i_s=1}^{3}\dot{\mathscr{L}}_{s_{i_s}}\\ \leq & -\lambda_d^2(x)-\theta^2\lambda_{\min}(Q)\|x\|^2-\|r\hat{\mu}^*(\widehat{x}_j)\|^2+\frac{\alpha_L}{2\varsigma}\|\nabla \mathscr{J}_L(x)\|\,\|C\|^2\left\|R^{-1}\right\|\lambda_2\\ &+\frac{1}{2}\|r\|^2\|R^{-1}\|^2\|C\|^2(K_{\delta_c}^2\left\|e_j\right\|^2\|\hat{w}_c\|^2+2\lambda_1^2\|\tilde{w}_c\|^2+2\lambda_2^2)-\frac{1}{4}(\nabla \hat{\mathscr{J}}^*(x))^{\mathsf{T}}\nabla \hat{\mathscr{J}}^*(x)\\ &+\frac{\Im}{2(1+\Im)^2}(\lambda_3^2-\lambda_{\min}(\sigma\sigma^{\mathsf{T}})\|\tilde{w}_c\|^2)-\frac{\alpha_L}{\varsigma}\lambda_{\min}(\mathscr{K})\|\nabla \mathscr{J}_L(x)\|^2\\ &-(1-\theta^2)\lambda_{\min}(Q)\|x\|^2\\ \triangleq & \,\pi_{\mathscr{L}_s}. \end{aligned} \tag{58}$$

If the SETC rule (46) and the weight-estimated error inequality (47) are satisfied, consider the following inequality:

$$\|\nabla \mathscr{J}_L(x)\| \geq \frac{\|C\|^2\left\|R^{-1}\right\|}{2\lambda_{\min}(\mathscr{K})}, \tag{59}$$

(58) becomes $\dot{\mathscr{L}}_s \leq -\theta^2\lambda_{\min}(Q)\|x\|^2$. It can be easily found that $\dot{\mathscr{L}}_s<0, \forall x\neq 0$.

Case 2: Performing the different operation to the Lyapunov function, we obtain

$$\Delta\mathscr{L}_s(t)=\mathscr{L}_3(\widehat{x}_{j+1})-\mathscr{L}_3(x(c_{j+1}^-))=\Delta\mathscr{L}_{s_1}(t)+\Delta\mathscr{L}_{s_2}(t)+\Delta\mathscr{L}_{s_3}(t). \tag{60}$$

Based on the analysis of Case 1, it can be concluded that $\dot{\mathscr{L}}_s(t)<0$ for all $t\in[c_j,c_{j+1})$. Moreover, the following result holds:

$$\Delta\mathscr{L}_{s_1}(t)=\mathscr{J}^*(\widehat{x}_{j+1})-\mathscr{J}^*(x(c_{j+1}^-))\leq 0, \tag{61}$$

$$\Delta\mathscr{L}_{s_2}(t)=\mathscr{J}^*(\widehat{x}_{j+1})-\mathscr{J}^*(\widehat{x}_j), \tag{62}$$

$$\begin{aligned}\Delta\mathscr{L}_{s_3}(t)=&\frac{1}{2\varsigma}\left(\tilde{w}_c^{\mathsf{T}}(\widehat{x}_{j+1})\tilde{w}_c(\widehat{x}_{j+1})-\tilde{w}_c^{\mathsf{T}}(x(c_{j+1}^-))\tilde{w}_c(x(c_{j+1}^-))\right)\\ &+\frac{\alpha_L}{\varsigma}\left(\mathscr{J}_L(\widehat{x}_{j+1})-\mathscr{J}_L(x(c_{j+1}^-))\right)\\ \leq & 0. \end{aligned} \tag{63}$$

For $\Delta\mathscr{L}_{s_2}(t)$, we have $\Delta\mathscr{L}_{s_2}(t)\leq-\mathscr{K}_1(\left\|e_{j+1}(c_j)\right\|)$, where $\mathscr{K}_1(\cdot)$ is a class-κ function [30] and $e_{j+1}(c_j)=\widehat{x}_{j+1}-\widehat{x}_j$. It can be observed that the Lyapunov function decreases monotonically for all times equal to c_{j+1}. By considering the triggering condition (46) and the

estimated error inequality (47), it can be concluded that the impulsive system in closed loop is asymptotically stable. Furthermore, the critic network's weight estimation error is UUB. Therefore, it concludes that the proof is completed. ■

5.3. Dynamic Event-Triggered Neural-Network-Based controller design

Based on the CNN, the internal dynamic variable can be denoted as

$$\begin{aligned}\dot{\eta}(x) =& -\alpha\eta(x) + (1-\theta^2)\lambda_{\min}(Q)\|x\|^2 + \frac{1}{4}(\nabla\hat{\mathscr{J}}^*(x))^{\mathsf{T}}\nabla\hat{\mathscr{J}}^*(x) + \lambda_d^2(x) \\ &+ \left\|r\hat{\mu}^*(\widehat{x}_j)\right\|^2 - \xi_{s_1}K_{\delta_c}\|\hat{w}_c\|^2\left\|e_j\right\|^2. \end{aligned} \tag{64}$$

Theorem 6 *The dynamic event-triggered control rule based on the critic network, incorporating Theorem 5, and the internal variable $\eta(x)$, ensure asymptotic stability of the closed-loop system and the error. Moreover, the weight error is guaranteed to be UUB. Its rule is defined as*

$$\left\|e_j\right\|^2 \leq \frac{\eta(x)}{\alpha_d\xi_{s_1}K_{\delta_c}\|\hat{w}_c\|^2} + \|\hat{e}_{T_s}\|^2 \triangleq \|\hat{e}_{T_d}\|^2, \tag{65}$$

where $\|\hat{e}_{T_d}\|$ is the DETC threshold based on the critic network.

Proof. We select a Lyapunov function $\mathscr{L}_d(t) = \mathscr{L}_s + \eta(x)$. Based on (64) and Theorem 5, it can be concluded that

$$\begin{aligned}\dot{\mathscr{L}}_d &= \dot{\mathscr{L}}_s + \dot{\eta}(x) \\ &\leq \pi_{\mathscr{L}_s} - \alpha\eta(x) + (1-\theta^2)\lambda_{\min}(Q)\|x\|^2 + \lambda_d^2(x) + \left\|r\hat{\mu}^*(\widehat{x}_j)\right\|^2 - \xi_{s_1}K_{\sigma_c}\|\hat{w}_c\|^2\left\|e_j\right\|^2. \end{aligned} \tag{66}$$

From inequalities (47) and (59), (66) becomes

$$\dot{\mathscr{L}}_d \leq -\alpha\eta(x) - \theta^2\lambda_{\min}(Q)\|x\|^2. \tag{67}$$

It can be obtained that $\dot{\mathscr{L}}_d < 0, \forall x \neq 0$. Therefore, the proof is ended. ■

Remark 3 *The occurrence of Zeno behavior, caused by the accumulation of events resulting from zero inter-execution time, cannot be ignored in the event-triggered control strategy. However, this issue can be prevented by ensuring that the minimum sampling time remains a positive constant, away from zero. In our study, by satisfying Assumption 4, we can ensure that the minimum sampling time is always greater than zero. This proof is similar to the one found in [31], which guarantees the exclusion of Zeno behavior.*

Remark 4 *By comparing the SETCS with the DETCS, several conclusions can be drawn. Firstly, unlike the SETC rule, the DETC rule involves a differential equation. Secondly, the DETC rule takes into account not only the current values of the state x and the error e_j, but also the previous values. Finally, the DETC threshold includes a dynamic variable, which distinguishes it from the SETC threshold that is solely dependent on time-varying factors.*

Table 1. Values of the Torsional Pendulum System.

Parameter	Meaning	Value
J	Rotary inertia	$1\,\mathrm{kg}\cdot 1^2$
M	Mass of the pendulum bar	$1/3\,\mathrm{kg}$
g	Gravitational acceleration	$9.8\,\mathrm{m/s^2}$
l	Length of the pendulum bar	$3/2\,\mathrm{m}$
f_d	Friction factor	0.2

6. Simulation

Consider a modified torsional pendulum disturbed system as

$$\begin{cases} \dot{x}_1 = x_2 + d(x) \\ \dot{x}_2 = \frac{1}{J}(u - Mgl\sin(x_1 + u) - f_d\dot{x}_1). \end{cases} \tag{68}$$

Values are referred to Table 1. Thus, it can be written as

$$\dot{x} = \begin{bmatrix} x_2 \\ -4.9\sin(x_1+u) - 0.2x_2 + u \end{bmatrix} + \begin{bmatrix} d(x) \\ -0.2d(x) \end{bmatrix}, \tag{69}$$

where the state vector $x = [x_1, x_2]^\mathsf{T} \in \mathbb{R}^2$, the control input $u \in \mathbb{R}$. Firstly, we need to carry on the system identification experiment. The initial value $x_0 = [1, -0.5]^\mathsf{T}$. We choose $a_1 = 1.25, a_2 = 1.5, a_3 = a_4 = 1.75, a_5 = 0.25$, and $m = 1$ for learning the dynamics. From Figure 1, the convergence process of identifier weight is displayed. It is obvious that the training effect is good. Final convergence values of weight matrices are shown in Table 2. It can be

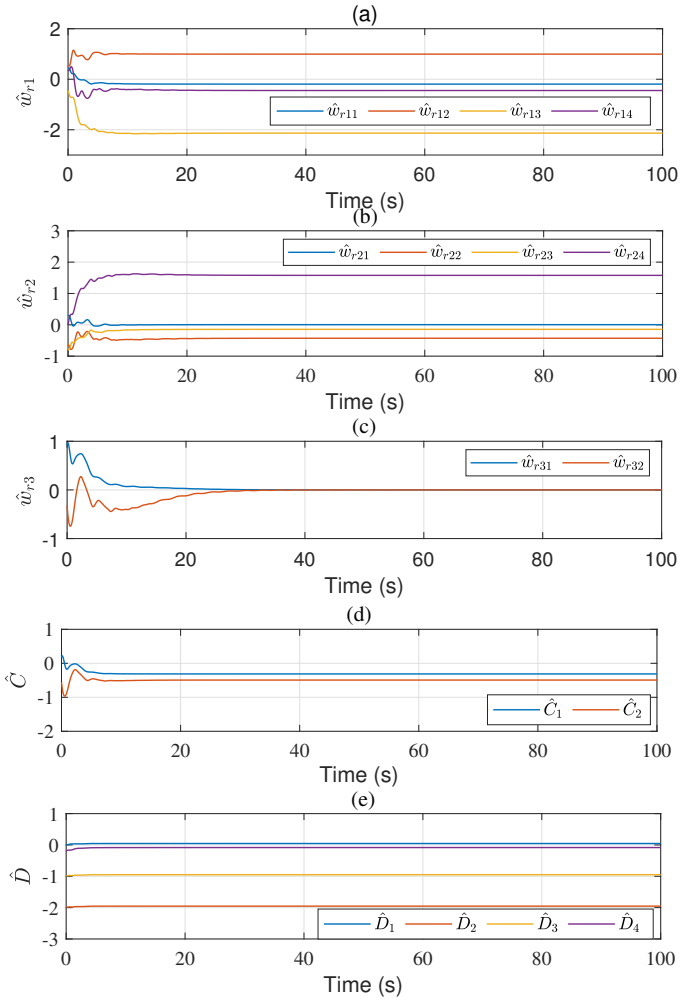

Figure 1. Convergence process of identifier weights.

observed that the identification error tends to zero value after a sufficient tuning state in Figure 2. Figure 3 is the 3D-view of the convergence process of $\tilde{x}_1$ and $\tilde{x}_2$, which can show changes more intuitively. Figure 4 shows the process of the system identification, where x_1, x_2 denote real states and $\hat{x}_1, \hat{x}_2$ represent approximate states. Note that our research object is a nominal system without the perturbed term at this step. Then, we use the affine model obtained after the RNN training to proceed to the next step.

Table 2. Values of RNN Weight.

Weights	Values			
$\hat{w}_{r1}$	-0.1927	0.9943	-2.1329	-0.4462
$\hat{w}_{r2}$	0.0050	-0.4285	-0.1453	1.5774
$\hat{w}_{r3}$	0	0		
$\hat{C}$	-0.3125	-0.4927		
$\hat{D}$	0.0463	-1.9525	-0.9491	-0.0831

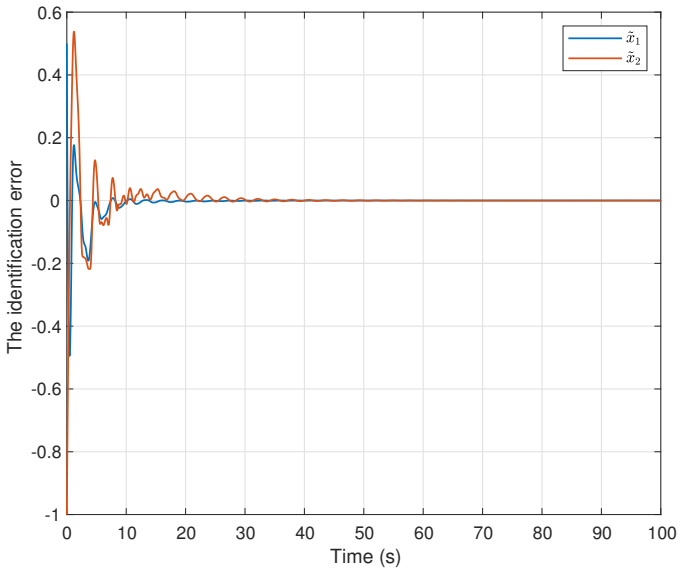

Figure 2. Identification error.

In this step, we conduct the ETC experiment. The CNN weight vector is $\hat{w}_c = [\hat{w}_{c1}, \hat{w}_{c2}, \hat{w}_{c3}]^{\mathsf{T}}$ and the activation function is $\delta(x) = [x_1^2, x_1x_2, x_2^2]^{\mathsf{T}}$. Set the learning rate $\varsigma = 0.2$, the designed parameter $\theta = 0.02$, the adjusting rate $\alpha_L = 0.05$, $\mathscr{J}_L(x) = 0.25x^{\mathsf{T}}x$, internal dynamic variable parameters $\alpha = 0.05, \alpha_d = 0.2$, the initial value $\eta(0) = 0$, and $K_{\delta_c} = 11$. The learning process of the critic network lasts for 300 s. The probing noise is active during the beginning 250s. Figure 5 shows the convergence of critic network weights. We set up a comparative experiment and select four different initial values of critic network weights. It is obvious that the final convergence values almost remain consistent. We select the initial value of critic network weights as zero. The critic network weight vector gradually tends to $[9.300, 3.162, 0.527]^{\mathsf{T}}$ after 200s. Subsequently, the data is fed into the dynamic variable (64) and triggering condition (65), and the resulting responses in the learning stage are illustrated in Figure 6. In this paper, we set 3000 samples. Figures 7 and 8 show the dynamic sampling period and triggering counts of the DETCS. Through calculation, it is determined that the dynamic triggering control law employs 614 samples. Figure 9 shows the spending samples of the SETCS, and its number is 1480. Obviously, the dynamic event-triggered controller costs fewer samples.

Then, we evaluate the robust stabilization of the system by using the approximate optimal control rule (40) with the disturbed term $d(x) = 0.5x_1\cos(x_2 - 1)$. We proceed to the next step with the trained critic network weights. The initial value of the state is $x_0 = [1, -0.5]^{\mathsf{T}}$. The state trajectory is shown in Figure 10, and its 3D visualization is presented in Figure 11. It is evident that the system exhibits the good robustness. Figure 12 depicts the control inputs obtained from the DETC and the time-triggered control formulations and Figure 13 illustrates the dynamic triggering condition employed in the control implementation. It is worth noting that the DETC input shows smaller fluctuations compared to the time-triggered

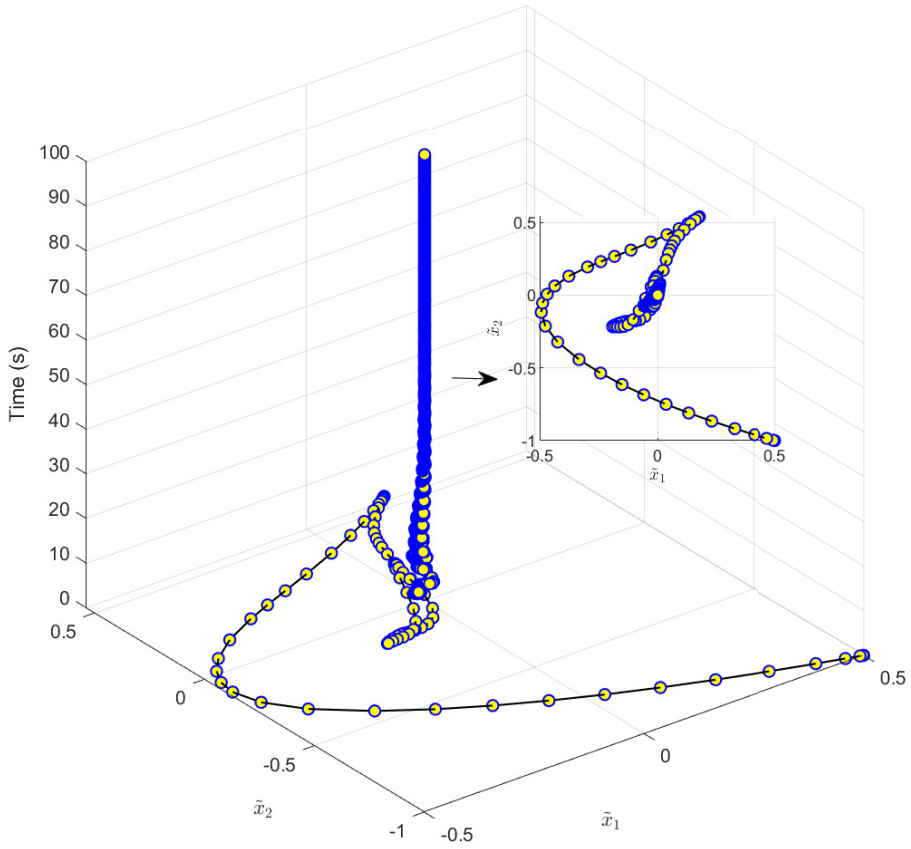

Figure 3. Identification error (3D-view).

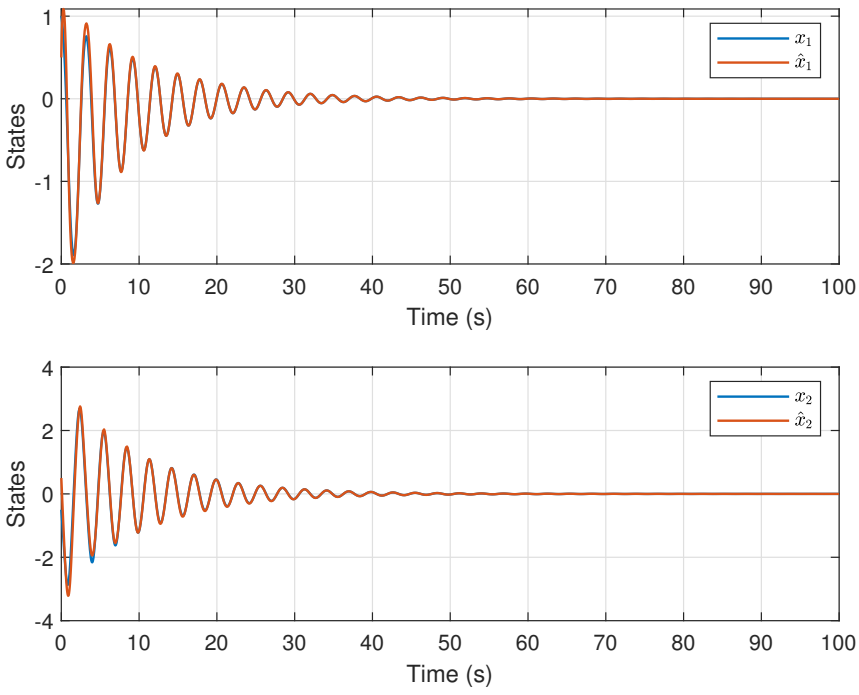

Figure 4. Learning process of the identification system.

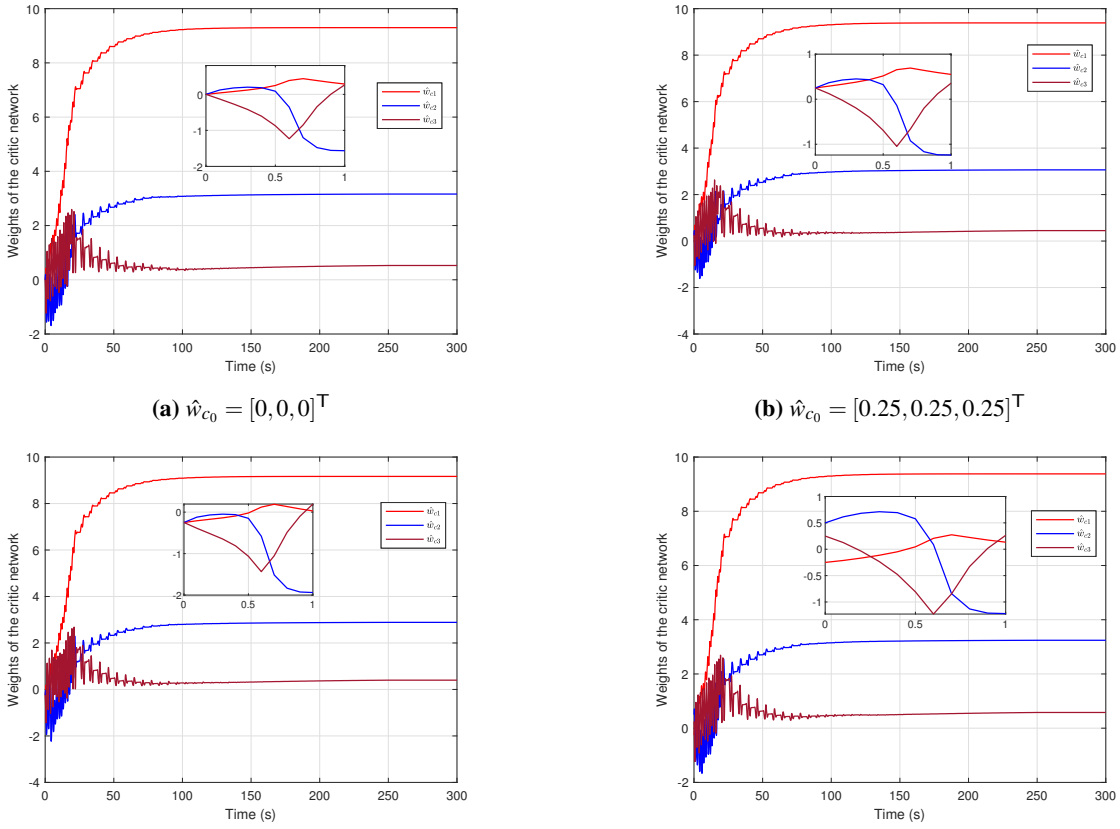

(a) $\hat{w}_{c_0} = [0,0,0]^{\mathsf{T}}$ **(b)** $\hat{w}_{c_0} = [0.25,0.25,0.25]^{\mathsf{T}}$

(c) $\hat{w}_{c_0} = [-0.25,-0.25,-0.25]^{\mathsf{T}}$ **(d)** $\hat{w}_{c_0} = [-0.25,0.50,0.25]^{\mathsf{T}}$

Figure 5. Convergence of critic network weights.

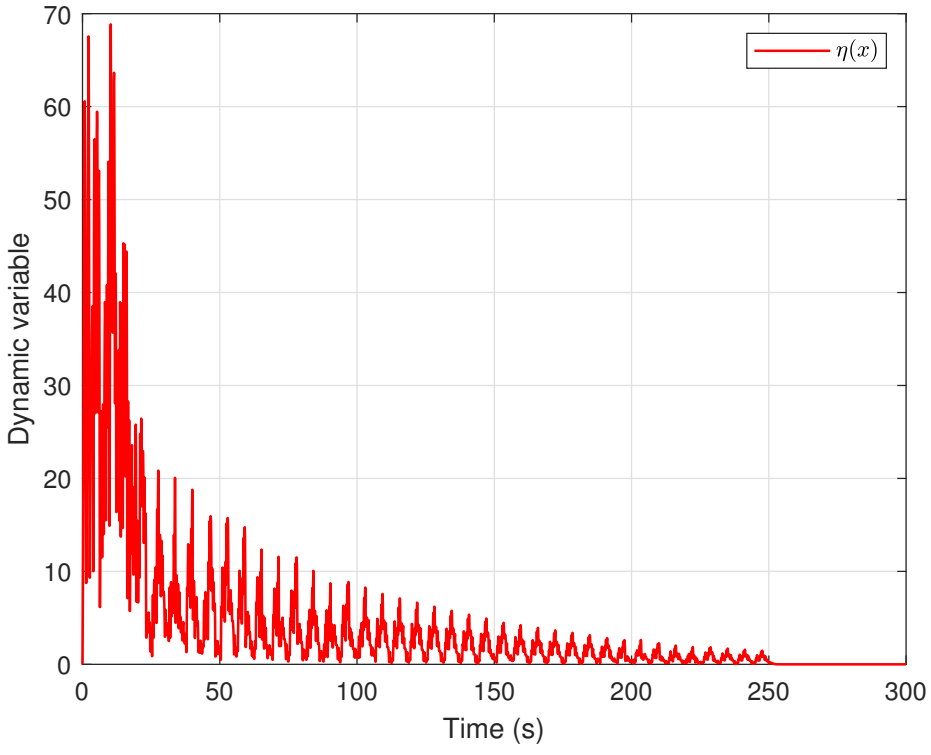

Figure 6. Response of the dynamic variable.

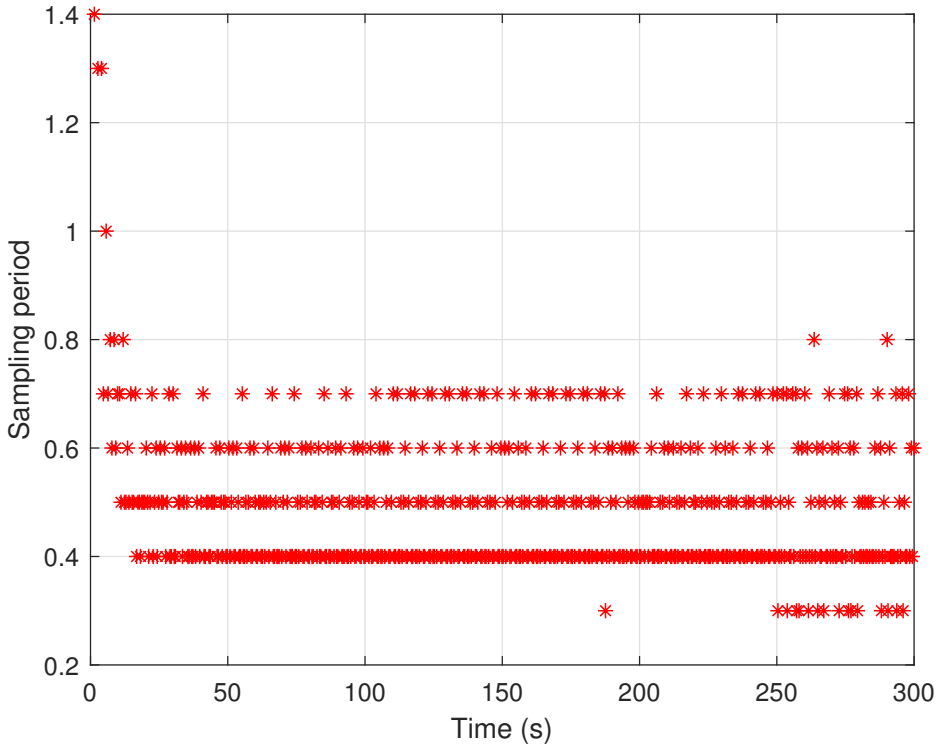

Figure 7. Dynamic sampling period.

control input. Moreover, the DETC input is only updated when the triggering condition is satisfied, resulting in lower updating frequency than the time-triggered control input. This reduces the computational load and communication burden between the controller and plant, which is an advantage in practical implementation. All these figures demonstrate the good effectiveness of the developed control.

7. Conclusion

This paper presents an improved DETCS for a class of CT non-affine nonlinear systems based on the CNN. We convert the robust control problem to an optimal control problem and construct a dynamic event-based controller with an internal dynamic variable, building on a static event-triggered controller. The DETC rule is updated only when the corresponding threshold condition is violated. Based on the critic network, we design an improved weight training rule to replace the traditional law to relax the selection range of initial values and design the dynamic event-based controller. At the same time, we demonstrate the stability of the closed-loop system. Finally, the feasibility and superiority of the designed scheme are demonstrated through a simulation experiment. It is worth noting that the paper mainly focuses on non-affine systems with matched uncertainties. Therefore, the design of DETCS for non-affine systems with general unmatched uncertainties requires further investigation.

Acknowledgments

This work was supported in part by the National Natural Science Foundation of China under Grant 62222301, Grant 61890930-5, and Grant 62021003; in part by the National Key Research and Development Program of China under Grant 2021ZD0112302, Grant 2021ZD0112301, and Grant 2018YFC1900800-5; and in part by the Beijing Natural Science Foundation under Grant JQ19013.

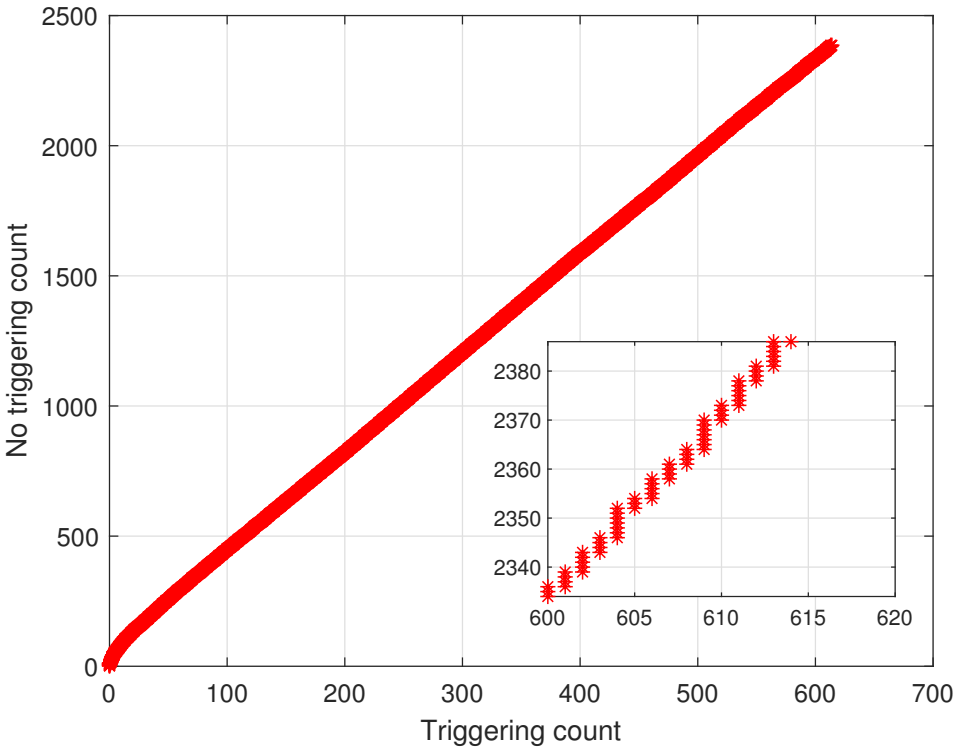

Figure 8. Triggering counts of dynamic event-triggered control.

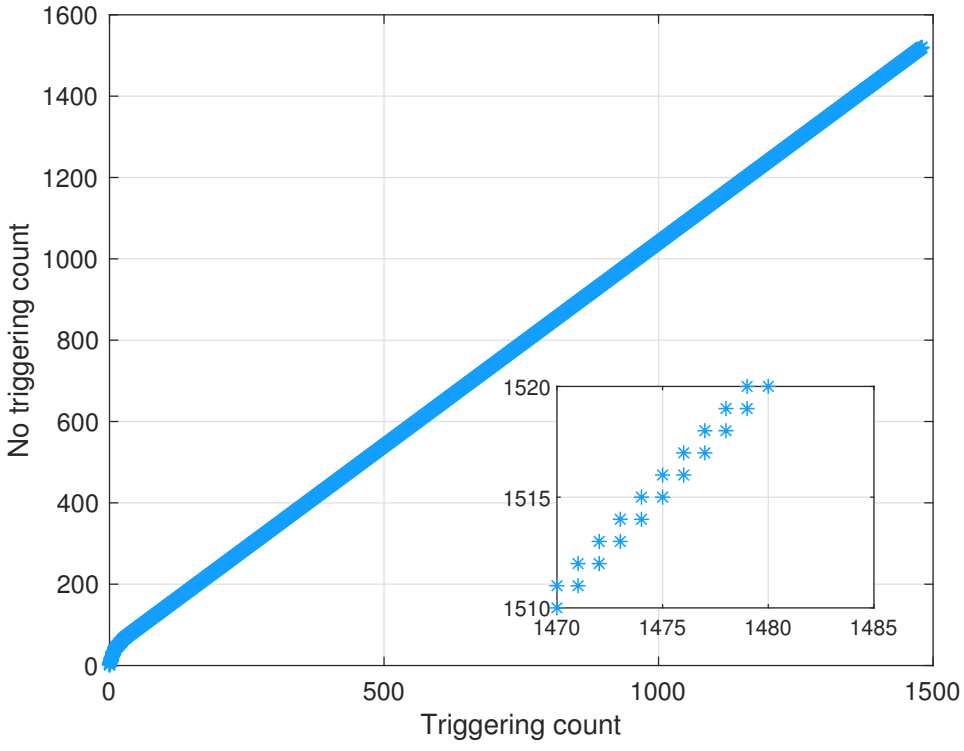

Figure 9. Triggering counts of static event-triggered control.

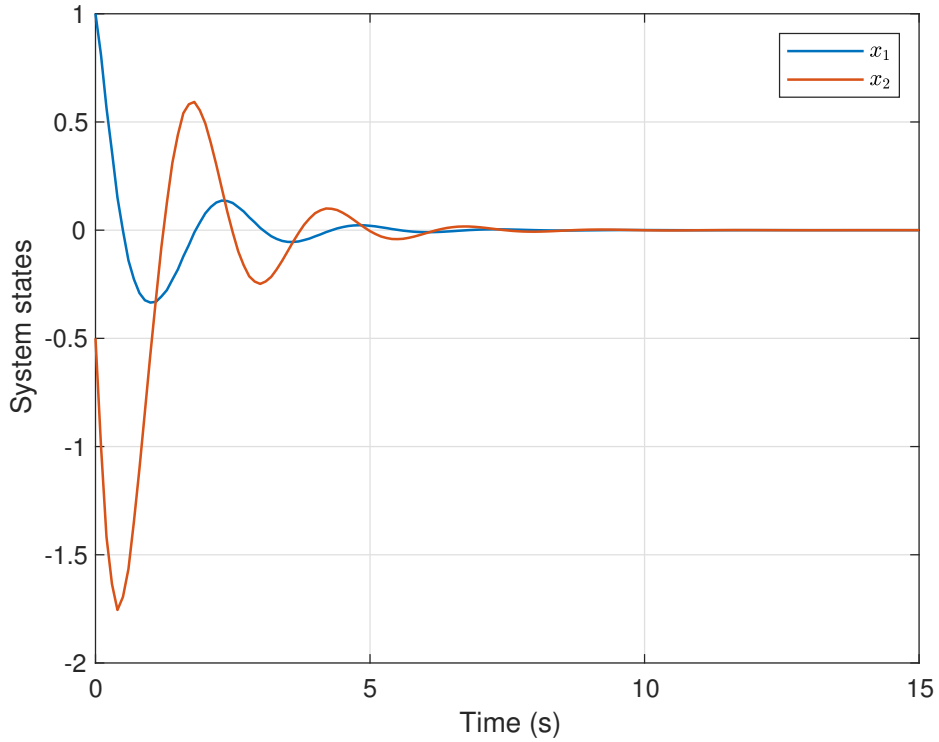

Figure 10. State trajectories.

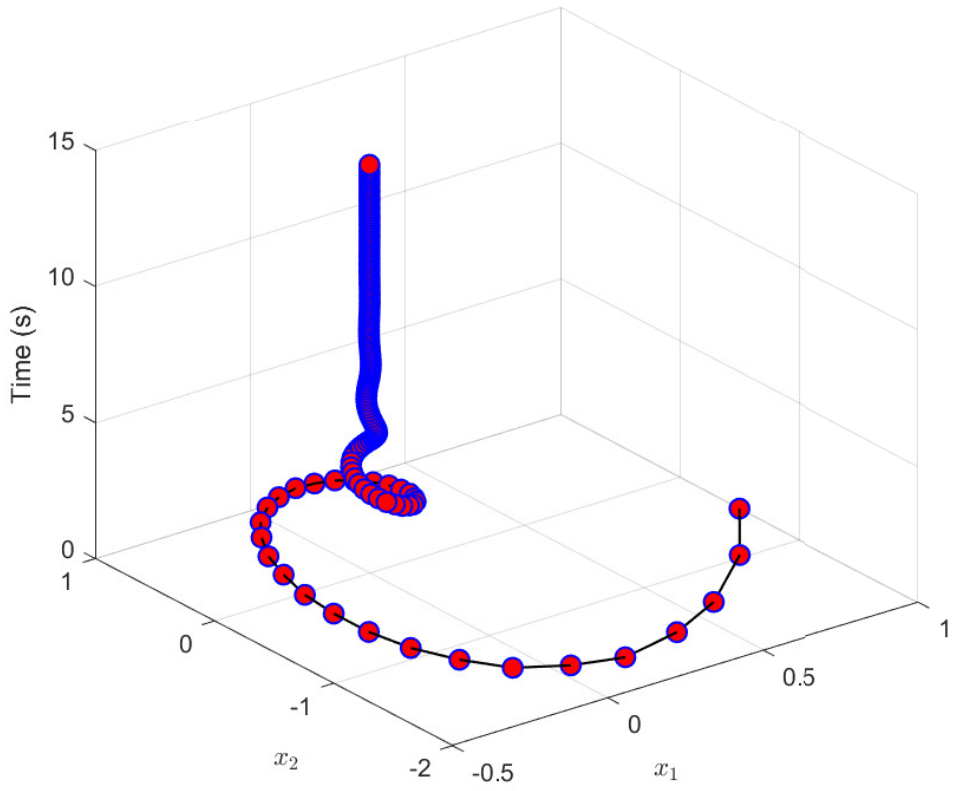

Figure 11. State trajectories (3D-view).

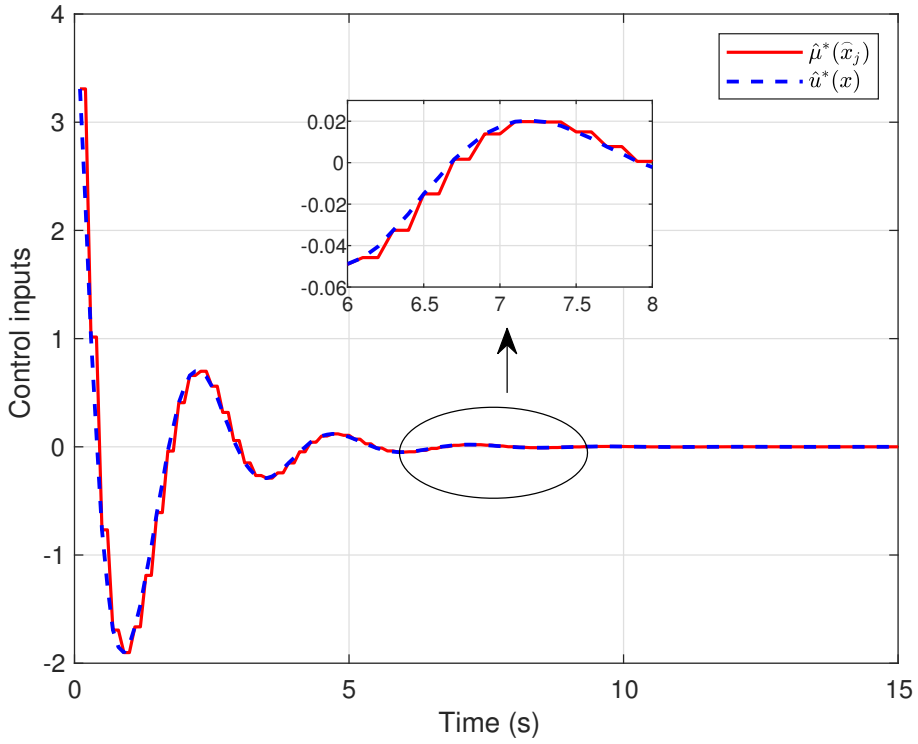

Figure 12. Control inputs based on dynamic event-triggered and time-triggered formulations.

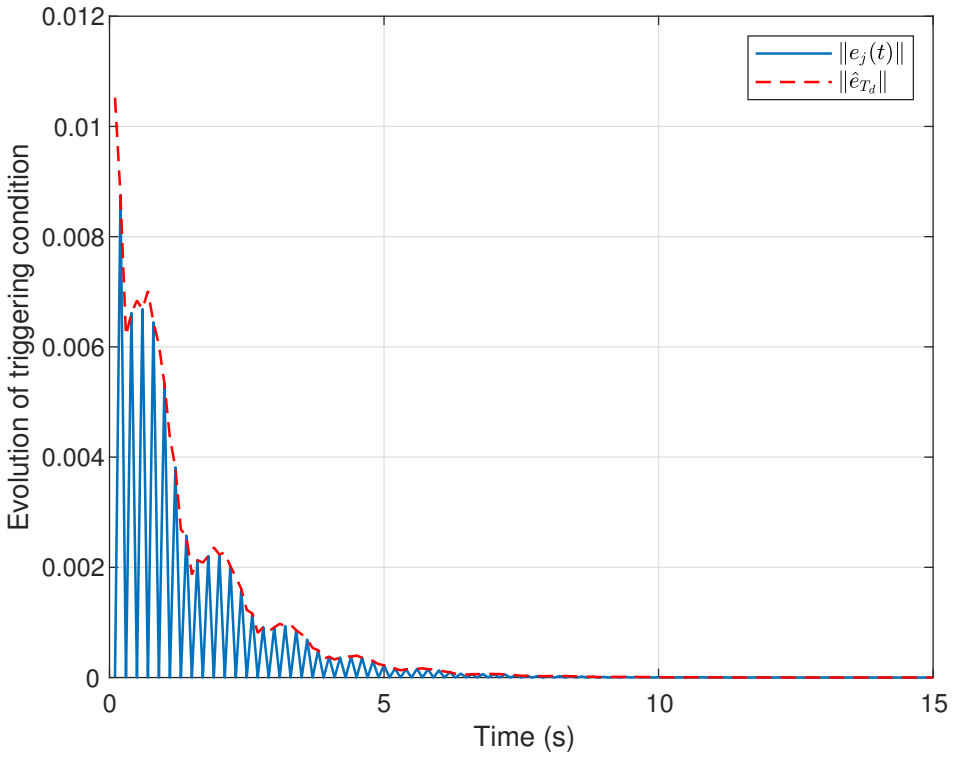

Figure 13. Dynamic triggering condition in the control implementation.

Conflicts of Interests

We confirm that there are no conflict of interests for this article.

Authors' Contribution

Zihang Zhou: Formal analysis; Validation; Writing - original draft; Ao Liu: Methodology; Supervision; Writing - review and editing; Ding Wang: Investigation; Supervision; Writing - review and editing.

References

[1] Wang D, Ha M, Zhao M. The intelligent critic framework for advanced optimal control. *AI Rev.* 2022, 55(1):1–22.

[2] Fan W, Liu A, Wang D. Decentralized tracking control design based on intelligent critic for an interconnected spring-mass-damper system. *Comp. Eng. Syst.* 2023, 3(1):5.

[3] Wang D, Wang J, Zhao M, Xin P, Qiao J. Adaptive multi-step evaluation design with stability guarantee for discrete-time optimal learning control. *IEEE/CAA J. Autom. Sinica* 2023, 10(9):1–13.

[4] Wang D, Wang J, Zhao M, Qiao J. Adaptive critic control design with knowledge transfer for wastewater treatment applications. *IEEE Trans. Ind. Inform.*, in press.

[5] Zhao M, Wang D, Qiao J, Ha M, Ren J. Advanced value iteration for discrete-time intelligent critic control: A survey. *AI Rev.*, in press.

[6] Ha M, Wang D, Liu D. Discounted iterative adaptive critic designs with novel stability analysis for tracking control. *IEEE/CAA J. Autom. Sinica* 2022, 9(7):1262–1272.

[7] Wang D, Hu L, Zhao M, Qiao J. Dual event-triggered constrained control through adaptive critic for discrete-time zero-sum games. *IEEE Trans. Syst., Man, Cybern., Syst.,* 2023, 53(3):1584–1595.

[8] Ming Z, Zhang H, Yan Y, Sun J. Self-triggered adaptive dynamic programming for model-free nonlinear systems via generalized fuzzy hyperbolic model. *IEEE Trans. Syst., Man, Cybern., Syst.,* 2023, 53(5):2792–2801.

[9] Xu Y, Jiang B, Yang H. Two-level game-based distributed optimal fault-tolerant control for nonlinear interconnected systems. *IEEE Trans. Neural Netw. Learn. Syst.* 2020, 31(11):4892–4906.

[10] Wang D, Zhao M, Ha M, Qiao J. Intelligent optimal tracking with application verifications via discounted generalized value iteration. *Acta Autom. Sinica* 2022, 48(1):182–193.

[11] Vamvoudakis K. Event-triggered optimal adaptive control algorithm for continuous-time nonlinear systems. *IEEE/CAA J. Autom. Sinica* 2014, 1(3):282–293.

[12] Guo X, Yan W, Cui R. Integral reinforcement learning-based adaptive NN control for continuous-time nonlinear MIMO systems with unknown control directions. *IEEE Trans. Syst., Man, Cybern., Syst.* 2020, 50(11):4068–4077.

[13] Wang D, Cheng L, Yan J. Self-learning robust control synthesis and trajectory tracking of uncertain dynamics. *IEEE Trans. Cybern.* 2022, 55(1):278–286.

[14] Wang D, Ren J, Ha M, Qiao J. System stability of learning-based linear optimal control with general discounted value iteration. *IEEE Trans. Neural Netw. Learn. Syst.* 2021.

[15] Lin F. *Robust Control Design: An Optimal Control Approach*. Wiley, 2007.

[16] D. Wang, D. Liu, H. Li. Policy iteration algorithm for online design of robust control for a class of continuous-time nonlinear systems. *IEEE Trans. Autom. Sci. Eng.* 2014, 11(2):627–632.

[17] Liu D, Xue S, Zhao B, Luo B, Wei Q. Adaptive dynamic programming for control: a survey and recent advances. *IEEE Trans. Syst., Man, Cybern.: Syst.* 2021, 51(1):142–160.

[18] Mu c, Wang K, Ni Z. Adaptive learning and sampled-control for nonlinear game systems using dynamic event-triggering strategy. *IEEE Trans. Neural Netw. Learn. Syst.* 2022, 33(9):4437–4450.

[19] Vamvoudakis K, Lewis F. Online actor-critic algorithm to solve the continuous-time infinite horizon optimal control problem. *Automatica* 2010, 46(5):878–888.

[20] Xue S, Luo B, Liu D. Event-triggered adaptive dynamic programming for unmatched uncertain nonlinear continuous-time systems. *IEEE Trans. Neural Netw. Learn. Syst.* 2021, 32(7):2939–2951.

[21] Song R, Wei Q, Zhang H, Lewis F. Discrete-time non-zero-sum games with completely unknown dynamics. *IEEE Trans. Cybern.* 2021, 51(6):2929-2943.

[22] Luo B, Yang Y, Liu D, Wu H. Event-triggered optimal control with performance guarantees using adaptive dynamic programming. *IEEE Trans. Neural Netw. Learn. Syst.* 2020, 31(1):76–88.

[23] Wang D. Intelligent critic control with robustness guarantee of disturbed nonlinear plants. *IEEE Trans. Cybern.* 2020, 50(6):2740–2748.

[24] Yang X, He H. Event-driven H_∞-constrained control using adaptive critic learning. *IEEE Trans. Cybern.* 2021, 51(10):4860–4872.

[25] Girard A. Dynamic triggering mechanisms for event-triggered control. *IEEE Trans. Autom. Control* 2015, 60(7):1992–1997.

[26] Liu K, Teel A, Sun X, Wang X. Model-based dynamic event-triggered control for systems with uncertainty: a hybrid system approach. *IEEE Trans. Autom. Control* 2021, 66(1):444-451.

[27] Wang D, Zhou Z, Li M, Ren J, Qiao J. Event-based robust performance guarantee for nonaffine plants via system identification. *Int. J. Robust Nonlinear Control* 2023, 33(10):5365-5387.

[28] Wang D, Mu C. Adaptive-critic-based robust trajectory tracking of uncertain dynamics and its application to a spring-mass-damper system. *IEEE Trans. Ind. Electron.* 2018 65(1):654–663.

[29] Modares H, Lewis F, Naghibi-Sistani M. Integral reinforcement learning and experience replay for adaptive optimal control of partially-unknown constrained-input continuous-time systems. *Automatica* 2014, 50(1):193–202.

[30] Khalil H, *Nonlinear Systems*. Upper Saddle River, NJ, USA: Prentice-Hall, 1996.

[31] Yang X, Wei Q. Adaptive critic learning for constrained optimal event-triggered control with discounted cost. *IEEE Trans. Neural Netw. Learn. Syst.* 2021, 32(1):91–104.